JOC Article

Multiple Conformational States in Crystals and in Solution in αγ Hybrid Peptides. Fragility of the C_{12} Helix in Short Sequences

Sunanda Chatterjee,[†] Prema G. Vasudev,[‡] Kuppanna Ananda,[†] Srinivasarao Raghothama,*[,§] Narayanaswamy Shamala,*[,‡] and Padmanabhan Balaram*[,†]

Molecular Biophysics Unit, Department of Physics, and NMR Research Centre, Indian Institute of Science, Bangalore-560012, India

pb@mbu.iisc.ernet.in; shamala@physics.iisc.ernet.in; sr@nrc.iisc.ernet.in

Received May 6, 2008

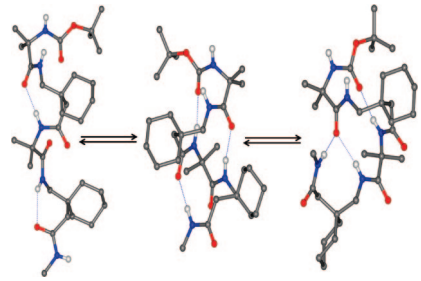

The conformational properties of foldamers generated from αγ hybrid peptide sequences have been probed in the model sequence Boc-Aib-Gpn-Aib-Gpn-NHMe. The choice of α-aminoisobutyryl (Aib) and gabapentin (Gpn) residues greatly restricts sterically accessible conformational space. This model sequence was anticipated to be a short segment of the αγ C_{12} helix, stabilized by three successive 4→1 hydrogen bonds, corresponding to a backbone-expanded analogue of the α polypeptide 3_{10}-helix. Unexpectedly, three distinct crystalline polymorphs were characterized in the solid state by X-ray diffraction. In one form, two successive C_{12} hydrogen bonds were obtained at the N-terminus, while a novel C_{17} hydrogen-bonded γαγ turn was observed at the C-terminus. In the other two polymorphs, isolated C_9 and C_7 hydrogen-bonded turns were observed at Gpn (2) and Gpn (4). Isolated C_{12} and C_9 turns were also crystallographically established in the peptides Boc-Aib-Gpn-Aib-OMe and Boc-Gpn-Aib-NHMe, respectively. Selective line broadening of NH resonances and the observation of medium range NH(i) ↔ NH(i+2) NOEs established the presence of conformational heterogeneity for the tetrapeptide in $CDCl_3$ solution. The NMR results are consistent with the limited population of the continuous C_{12} helix conformation. Lengthening of the $(\alpha\gamma)_n$ sequences in the nonapeptides Boc-Aib-Gpn-Aib-Gpn-Aib-Gpn-Aib-Gpn-Xxx (Xxx = Aib, Leu) resulted in the observation of all of the sequential NOEs characteristic of an αγ C_{12} helix. These results establish that conformational fragility is manifested in short hybrid αγ sequences despite the choice of conformationally constrained residues, while stable helices are formed on chain extension.

Introduction

Hybrid polypeptides which incorporate the higher homologues of the α amino acids provide an entry to a new class of hydrogen-bonded peptide structures.[1] The area of foldamer design has received great impetus from the realization that β- and γ-amino acid residues can be accommodated into folded structures like helices and hairpins, thereby providing a route to generate synthetic mimics of protein structures.[1c,2] Several unique structural features of polypeptide backbones containing the higher homologues of α amino acids have been established by extensive studies of oligo-β- and -γ-peptides.[3] Hybrid peptide design is facilitated by the use of stereochemically constrained amino acids in which the range of accessible conformations is limited by backbone substitution. For α residues, the most widely used constrained residue is α-aminoisobutyric acid (Aib).[4] We have recently described the introduction of the achiral, β,β-disubstituted γ amino acid residue gabapentin (Gpn,

* To whom correspondence should be addressed. Fax: (P.B.) 91-80-23600683/91-80-23600535; (N.S.) 91-80-23602602/91-80-23600683.
[†] Molecular Biophysics Unit.
[‡] Department of Physics.
[§] NMR Research Centre.

10.1021/jo8009819 CCC: $40.75 © 2008 American Chemical Society
Published on Web 07/29/2008

SCHEME 1. Definition of the Backbone Torsion Angles of the Gpn Residue

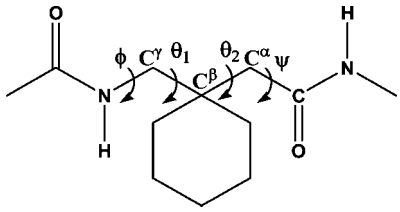

1-(aminomethyl)cyclohexaneacetic acid) as a model residue in the design of hybrid peptides.[5] The geminal β substituents in Gpn restrict the backbone torsion angles $C^{\beta}-C^{\gamma}$ (θ_1) and $C^{\alpha}-C^{\beta}$ (θ_2) to *gauche* ($\theta = \pm 60°$) conformations, thereby restricting the range of energetically feasible conformations (Scheme 1.)[5] Despite the limitations placed on θ_1 and θ_2, hybrid $\alpha\gamma$ sequences containing Gpn have a much wider range of conformational choices than their $\alpha\alpha$ counterparts. Indeed, several intramolecular hydrogen bond stabilized conformations like the C_7 (NH(i)→CO(i)) and C_9 (CO($i-1$)←NH($i+1$), where Gpn is the ith residue) structures have been characterized at the Gpn residues in di- and tripeptides.[5a] One regular structure has been observed in crystals for $\alpha\gamma$ hybrid sequences in the tetrapeptide Boc-Aib-Gpn-Aib-Gpn-OMe (**1**).[1d] This is the $\alpha\gamma$ C_{12} helix which may be viewed as the expanded hybrid peptide analogue of the classical 3_{10}-helix observed in α peptides.[4b,6] The observation of a consecutive C_{12} hydrogen-bonded structure, corresponding to one turn of a regular $\alpha\gamma$ C_{12} helix, in peptide **1** (Figure 1a) prompted us to explore the possibility of an extension of such a helical structure by introduction of an additional hydrogen bond donor at the C-terminus (Figure 1b).

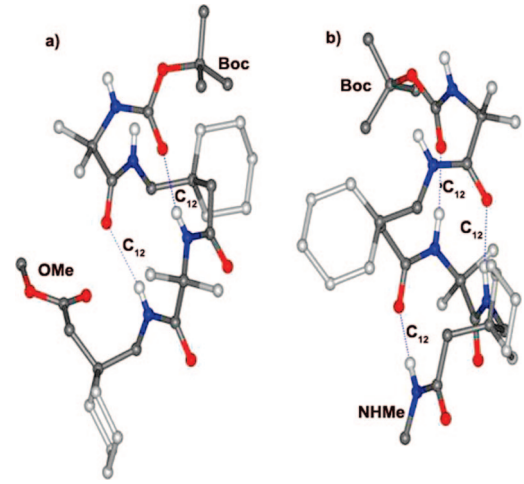

FIGURE 1. (a) Molecular conformation of Boc-Aib-Gpn-Aib-Gpn-OMe (**1**) determined in crystals.[1d] (b) Anticipated conformation of Boc-Aib-Gpn-Aib-Gpn-NHMe (**2**), stabilized by three consecutive C_{12} hydrogen bonds. Model is based on the conformation in Figure 1(a) by fixing Gpn (4) torsion angles to the same value as Gpn (2).

This apparently minor structural modification resulted in the observation of unexpected structures, providing new insights into the accessible conformations for $\alpha\gamma$ sequences containing the conformationally constrained Gpn residue. We describe in this report the conformational characterization of the peptide Boc-Aib-Gpn-Aib-Gpn-NHMe (**2**) and extension of the $\alpha\gamma$ segment in the nonapeptides Boc-Aib-Gpn-Aib-Gpn-Aib-Gpn-Aib-Gpn-Xxx-OMe (Xxx = Aib (**3**) and Xxx = Leu (**4**)). Interestingly, **2** crystallized in three different polymorphic forms permitting characterization of distinctly different backbone conformations stabilized by intramolecular C_7, C_9, and C_{12} hydrogen bonds. An unanticipated C_{17} hydrogen bond stabilizing a three-residue $\gamma\alpha\gamma$ turn has also been observed. Solution NMR studies support the presence of multiple conformational states and averaging by exchange effects as revealed by the presence of distinctive medium range NOEs between backbone NH protons and selective line broadening. Lengthening of the polypeptide chain stabilizes the C_{12} helix as revealed by NMR studies of the nonapeptides **3** and **4**.

Results

Crystalline Polymorphs of Peptide 2. Figure 2 illustrates the observed conformations of peptide **2** in distinct polymorphic forms. The relevant backbone torsional angles and intramolecular hydrogen bond parameters in polymorphs **2a**−**c** are listed in Tables 1 and 2, respectively. The two molecules in the asymmetric unit of **2a** in the space group $P2_1/c$ adopt *almost identical* backbone (mirror image) conformations, with the Aib-Gpn-Aib segment forming two consecutive $\alpha\gamma/\gamma\alpha$ turns resulting in an incipient C_{12} helix, which can be formally considered as a backbone-expanded analogue of the 3_{10} (C_{10})-helix.[6a,b] The C-terminus adopts a folded conformation resulting in a C_{17} hydrogen bond between the Aib (1) CO and methylamide NH groups. The Aib (1) CO group participates in a bifurcated hydrogen bond interaction with two donor groups, NHMe and Gpn (4) NH. The two independent molecules in the asymmetric unit differ in the orientation of the geminal substituents on the cyclohexane ring of the Gpn (4) residue. Polymorphs **2b** and **2c** reveal a completely different backbone conformation. In both

(1) (a) Chatterjee, S.; Roy, R. S.; Balaram, P. *J. R. Soc. Interface* **2006**, *4*, 587–606. (b) Roy, R. S.; Balaram, P. *J. Peptide Res.* **2004**, *63*, 279–289. (c) Karle, I. L.; Pramanik, A.; Banerjee, A.; Battacharjya, S.; Balaram, P. *J. Am. Chem. Soc.* **1997**, *119*, 9087–9095. (d) Ananda, K.; Vasudev, P. G.; Sengupta, A.; Raja, K. M. P.; Shamala, N.; Balaram, P. *J. Am. Chem. Soc.* **2005**, *127*, 16668–16674. (e) Baldauf, C.; Gunther, R.; Hofmann, H. J. *Biopolymers* **2006**, *84*, 408–413. (f) Baldauf, C.; Gunther, R.; Hofmann, H. J. *J. Org. Chem.* **2006**, *71*, 1200–1208. (g) Schmitt, M. A.; Choi, H. S.; Guzei, I. A.; Gellman, S. H. *J. Am. Chem. Soc.* **2005**, *127*, 13130–13131. (h) Schmitt, M. A.; Choi, H. S.; Guzei, I. A.; Gellman, S. H. *J. Am. Chem. Soc.* **2006**, *128*, 4538–4539.

(2) (a) Rai, R.; Balaram, P. In *Foldamers: Structure, Properties and Applications*; Hecht, S., HucI. Eds.; Wiley-VCH Verlag GmbH & Co.: New York, 2007; pp 147−171. (b) Goodman, C. M.; Choi, S.; Shandler, S.; DeGrado, W. F. *Nature Chem. Biol.* **2007**, *3*, 252–262. (c) Karle, I. L.; Gopi, H. N.; Balaram, P. *Proc. Natl. Acad. Sci. U.S.A.* **2002**, *99*, 5160–5164. (d) Roy, R. S.; Gopi, H. N.; Raghothama, S.; Karle, I. L.; Balaram, P. *Chem. Eur. J.* **2006**, *12*, 3295–3302.

(3) (a) Gellman, S. H. *Acc. Chem. Res.* **1998**, *31*, 173–180. (b) Seebach, D.; Beck, A. K.; Bierbaum, D. J. *Chem. Biodiversity* **2004**, *1*, 1111–1239. (c) Seebach, D.; Hook, D. F.; Glattli, A. *Biopolymers* **2006**, *84*, 23–37. (d) Cheng, R. P.; Gellman, S. H.; DeGrado, W. F. *Chem. Rev.* **2001**, *101*, 3219–3232. (e) Hanessian, S.; Luo, X.; Schaum, R.; Michnick, S. *J. Am. Chem. Soc.* **1998**, *120*, 8569–8570. (f) Hanessian, S.; Luo, X.; Schaum, R. *Tetrahedron Lett.* **1999**, *40*, 4925–4929. (g) Grotenberg, G. M.; Timmer, M. S. M.; Llamas-Siaz, A. L.; Verdoes, M.; van der Marel, G. A.; van Raaij, M. J.; Overkleeft, H. S.; Overhand, M. S. *J. Am. Chem. Soc.* **2004**, *126*, 3444–3446.

(4) (a) Prasad, B. V. V.; Balaram, P. *CRC Crit. Rev. Biochem.* **1984**, *16*, 307–347. (b) Karle, I. L.; Balaram, P. *Biochemistry* **1990**, *29*, 6747–6756. (c) Venkatraman, J.; Shankaramma, S. C.; Balaram, P. *Chem. Rev.* **2001**, *101*, 3131–3152. (d) Aravinda, S.; Shamala, N.; Roy, R. S.; Balaram, P. *Proc. Indian Acad. Sci. (Chem. Sci.)* **2003**, *115*, 373–400. (e) Toniolo, C.; Benedetti, E. *Macromolecules* **1991**, *24*, 4004–4009. (f) Crisma, M.; Formaggio, F.; Toniolo, C.; Moretto, A. *Biopolymers (Peptide Sci.)* **2006**, *84*, 3–12.

(5) (a) Vasudev, P. G.; Ananda, K.; Chatterjee, S.; Aravinda, S.; Shamala, N.; Balaram, P. *J. Am. Chem. Soc.* **2007**, *129*, 4039–4048. (b) Ananda, K.; Aravinda, S.; Vasudev, P. G.; Raja, K. M. P.; Sivaramakrishnan, H.; Nagarajan, K.; Shamala, N.; Balaram, P. *Curr. Sci.* **2003**, *85*, 1002–1011. (c) Banerjee, A.; Balaram, P. *Curr. Sci.* **1997**, *73*, 1067–1077, and ref 3d.

(6) (a) Donohue, J. *Proc. Natl. Acad. Sci. U.S.A.* **1953**, *39*, 470–478. (b) Toniolo, C.; Benedetti, E. *Trends Biochem. Sci.* **1991**, *16*, 350–353. (c) For a discussion on the relationship between the hydrogen-bonded structures observed in $\alpha\alpha$ and $\alpha\gamma$ segments, see ref 1a.

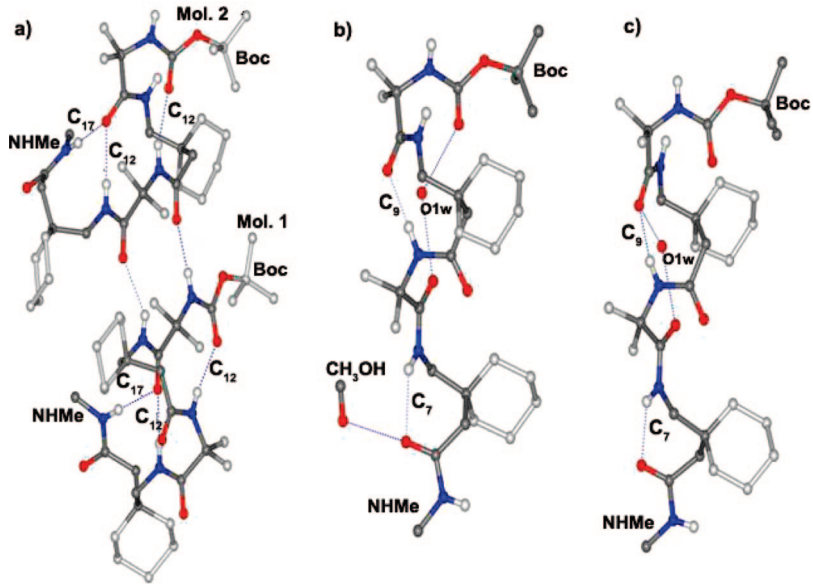

FIGURE 2. Molecular conformation of Boc-Aib-Gpn-Aib-Gpn-NHMe (**2**) in three polymorphic crystals: (a) polymorph **2a**, (b) polymorph **2b**, and (c) polymorph **2c**. rmsd for backbone superposition of **2b** and **2c** is 0.12 Å.

TABLE 1. Backbone Torsion Angles (deg) for Peptides 2, 5, and 6[a]

	2a (mol. 1)					**2a** (mol. 2)				
residue	ϕ	θ_1	θ_2	ψ	ω	ϕ	θ_1	θ_2	ψ	ω
Aib (1)	59.3			43.0	174.4	−57.8			−38.4	−174.5
Gpn (2)	127.9	−55.3	−62.1	112.9	176.2	−129.2	53.0	63.3	−108.9	−176.5
Aib (3)	53.1			48.7	174.7	−50.8			−51.4	179.8
Gpn (4)	−105.7	−63.4	−64.8	108.4	178.0	108.9	64.2	62.3	−104.9	−177.1
	2b					**2c**				
residue	ϕ	θ_1	θ_2	ψ	ω	ϕ	θ_1	θ_2	ψ	ω
Aib (1)	−53.1			−46.2	−174.8	−59.0			−45.9	−177.3
Gpn (2)	−106.9	63.9	75.7	−77.4	−174.7	−99.7	68.4	73.8	−76.9	−173.0
Aib (3)	58.4			−148.3	−173.4	57.1			−146.3	−175.3
Gpn (4)	−103.8	−46.8	−50.1	−121.1	−174.7	−104.4	−45.1	−47.5	−123.6	−174.2
	5 (mol. 1)					**5** (mol. 2)				
residue	ϕ	θ_1	θ_2	ψ	ω	ϕ	θ_1	θ_2	ψ	ω
Aib (1)	60.6			33.8	176.9	−57.5			−38.7	−174.9
Gpn (2)	128.0	−56.3	−59.1	116.7	−176.7	−131.9	55.3	61.5	−110.4	179.0
Aib (3)	−52.7			−47.9	−173.3	49.2			49.8	175.9

	6				
residue	ϕ	θ_1	θ_2	ψ	ω
Gpn (1)	−102.3	66.1	75.1	−81.4	−173.5
Aib (2)	−60.5			−49.4	−173.3

[a] The choice of sign is arbitrary and represents one enantiomeric form present in the centrosymmetric crystals. For convenience, the "−" signs of the ϕ, ψ values have been chosen, since this corresponds to the observed handedness in the case of peptides formed by L-amino acids. In the case of **2a** and **5**, the two molecules in the asymmetric unit have opposite handedness. Estimated standard deviations ∼1° (**2a**), 0.2° (**2b**), 0.6° (**2c**), and 0.5° (**5**, **6**).

cases, the Gpn (2) adopts a C_9 conformation, while Gpn (4) adopts a C_7 conformation. Notably, in both the cases, Aib (3) residue adopts an unusual polyproline II (P_{II}) conformation ($\phi \approx -60°$ and $\psi \approx +120°$). The Aib residue has been shown to adopt helical conformations ($3_{10}/\alpha$, $\phi = \pm 60°$, $\psi = \pm 30°$), in a very large number of peptides characterized so far by X-ray diffraction.[4] A lone water molecule bridges the Boc CO and Aib (3) CO groups in **2b**. In **2c**, the water bridge is between Aib (1) CO and Aib (3) CO groups (Table 2). The water molecule forms two strong hydrogen bonds to the acceptor carbonyl groups in **2c**, whereas in **2b**, one of the hydrogen bonds appears distinctly weaker (O···H = 2.51 Å). Polymorphs **2b** and **2c** have very similar backbone conformations and differ only in the presence of a methanol molecule (occupancy 0.25) in the crystals of the former. **2a** and **2b**/**2c** are conformational polymorphs, whereas **2b** and **2c** differ only in solvation.[7] The three-residue $\gamma\alpha\gamma$ turn (**2a**) stabilized by a 17-atom (C_{17}) hydrogen bond results in the formation of a reverse turn structure, bringing $C^{\alpha}(i)$ and $C^{\alpha}(i+4)$ into proximity (5.2 Å, Figure 3a.) Inspection of the torsion angles in Table 1 reveals that the formation of the C_{17} structure requires the Gpn (2) and Gpn (4) residues to

TABLE 2. Intramolecular Hydrogen-Bond Parameters in Peptides 2, 5, and 6

type	donor (D)	acceptor (A)	D···A (Å)	H···A (Å)	∠D−H···A (°)
		2a (mol. 1)			
C_{12}	N3	O0	2.93	2.08	167.8
C_{12}	N4	O1	2.93	2.08	171.3
C_{17}	N5	O1	2.88	2.02	174.0
		(mol. 2)			
C_{12}	N3	O0	2.91	2.09	159.9
C_{12}	N4	O1	3.07	2.21	179.0
C_{17}	N5	O1	2.97	2.11	175.2
		2b			
C_9	N3	O1	2.86	1.95	177.5
C_7	N4	O4	2.87	2.22	126.8
	O1w	O3	2.81	2.01	165.9
	O1w	O0	3.10	2.51	135.9
		2c			
C_9	N3	O1	2.85	1.96	168.9
C_7	N4	O4	2.77	2.08	133.6
	O1w	O1	2.93	2.07	163.9
	O1w	O3	2.80	2.02	167.8
		5 (mol. 1)			
C_{12}	N3	O0	3.04	2.19	171.7
		(mol. 2)			
C_{12}	N3	O0	2.97	2.12	172.9
		6			
C_9	N2	O0	2.83	2.02	175.9

adopt unique local conformations with distinct ϕ values (Gpn (2), $\phi = 127.9°$ (mol. 1) and $-129.2°$ (mol. 2); Gpn (4), $\phi = -105.7°$ (mol. 1) and 108.9° (mol. 2)).

Conformations in Crystals of Isolated αγ and γα Units. In order to evaluate the conformational propensities and stabilities of Aib-Gpn and Gpn-Aib segments, the crystal structures of Boc-Aib-Gpn-Aib-OMe (**5**) and Boc-Gpn-Aib-NHMe (**6**) were determined. The molecular conformations are shown in Figure 4, and the backbone conformational angles and hydrogen bond parameters are summarized in Tables 1 and 2, respectively. In **5**, the Aib-Gpn segment adopts a helical C_{12} turn in both molecules in the asymmetric unit. In contrast, the Gpn-Aib segment in **6** does not reveal the formation of a C_{12} hydrogen bond. Rather, the Gpn residue adopts a C_9 hydrogen bonded conformation, which can be formally viewed as an expanded version of the C_7 (γ-turn) feature observed in α peptide structures.[8] The N···O distance between the groups Boc CO and NHMe, which were expected to form a C_{12} hydrogen bond in this structure, is 5.0 Å. Notably, the backbone torsion angles for both the Gpn and Aib residues are not very far from the values which will result in a C_{12} hydrogen bond. From the data presented in Table 1, it is observed that relatively small changes of approximately 25° of Gpn ϕ and 30° of Gpn ψ result in a transformation of the C_{12} turn into the C_9 hydrogen bond, which is a localized interaction determined only by the torsion angles at Gpn.

Solution Conformations of Boc-Aib-Gpn-Aib-Gpn-NHMe (2). Figure 5 shows the 500 MHz NMR spectrum of **2** in $CDCl_3$ at 300 K. A notable feature of the spectrum is the selective broadening of the amide NH resonances of Gpn (2) and methyl amide NH groups. The inset to Figure 5 illustrates the effect of raising and lowering of temperature. Broadening is distinctly more pronounced for the methylamide group upon heating and cooling, in addition to large chemical shift changes. This behavior suggests that exchange between multiple conformations separated by widely different activation barriers is present in solution. Figure 6 shows a partial ROESY spectrum of peptide **2** in $CDCl_3$. Inspection of the NOEs observed between backbone NH protons reveals both sequential and medium range d_{NN} NOEs. The d_{NN} 1↔2, 2↔3, and 3↔4 NOEs are indeed observed in Figure 6, supporting formation of C_{12} helical turns over the Aib(1)-Gpn(2)-Aib(3) segment. Indeed, expected NH(i) ↔ NH(i+1) distance in a C_{12} helix are $d_{NN}(\alpha\gamma) = 2.7$ Å and $d_{NN}(\gamma\alpha) = 3.4$ Å. This is further elaborated in the discussion on the nonapeptide **3**. No detectable NOE was observed between Gpn (4) NH and the methylamide NH protons, suggesting the absence of the third helical C_{12} turn. In the observed crystal structure of polymorph **2a** this interproton distance is 2.7 Å, suggesting that in solution the novel C_{17}-turn conformation may be populated only to a limited extent.

The following medium-range d_{NN} NOEs are also observed: Aib (1) NH ↔ Aib (3) NH and Gpn (2) NH ↔ Gpn (4) NH. The corresponding interproton distances in the C_{12} helix are 4.7 and 4.6 Å, respectively, which are beyond the distance limits for efficient interproton dipolar interactions. Consequently, these NOEs must arise from a distinctly different set of peptide conformations. The medium-range NOEs may be rationalized by considering an alternative "*non-helical*" conformation stabilized by two C_{12} hydrogen bonds (Figure 3b). In this structure, the Aib(1)-Gpn(2) segment forms a "*non-helical*" C_{12} turn which has been built using allowed, crystallographically characterized conformations of Aib and Gpn residues, resulting in an interproton distance of 3.8 Å between Aib (1) NH and Aib (3) NH and an interproton distance of 2.9 Å between Gpn (2) NH and Gpn (4) NH. This structure is stabilized by two intramolecular hydrogen bonds. Indeed, the local residue conformation used in this model for Gpn (1) is crystallographically observed for Gpn (4) in polymorph **2a**.

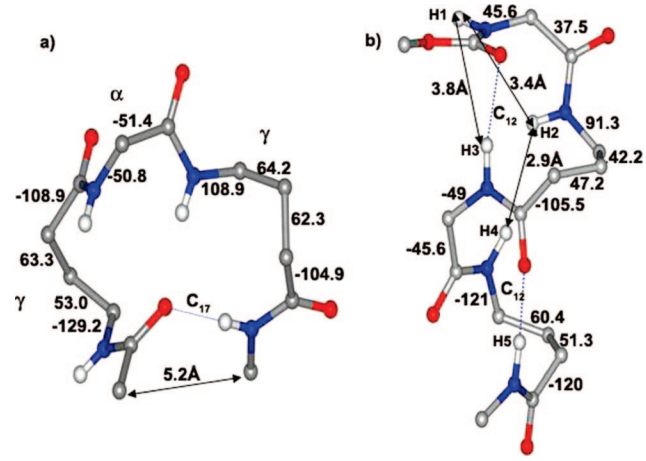

FIGURE 3. (a) The γαγ C_{17} turn observed in the crystal structure of Boc-Aib-Gpn-Aib-Gpn-NHMe (**2a**, **-**Gpn(2)-Aib(3)-Gpn(4)- segment of mol. 2). Backbone torsion angles determining the turn are indicated. (b) An alternate conformation of the tetrapeptide **2**, generated by selecting the allowed/crystallographically observed backbone torsion angles for Aib and Gpn residues, which explains the medium range NOEs shown in Figure 6.

(7) (a) The terms conformational polymorphs, pseudopolymorphs, and solvates have attracted considerable debate in the literature of organic solid-state chemistry. When considering molecular arrangements in crystals of relatively large molecules like oligopeptides, a precise application of these terms may be inappropriate. For a discussion on polymorphism in organic crystals, see ref , and for a recent discussion on conformational polymorphism in small organic molecules, see ref 8c. (b) Bernstein, J. *Polymorphism in Molecular Crystals*; Oxford University Press: Oxford, 2002. (c) Nangia, A. *Acc. Chem. Res.* **2008**, *41*, 595–604.

(8) (a) Matthews, B. W. *Macromolecules* **1972**, *5*, 818–819. (b) Némethy, G.; Printz, M. P. *Macromolecules* **1972**, *5*, 755–758. (c) Milner-White, E. J. *J. Mol. Biol.* **1990**, *216*, 385–397.

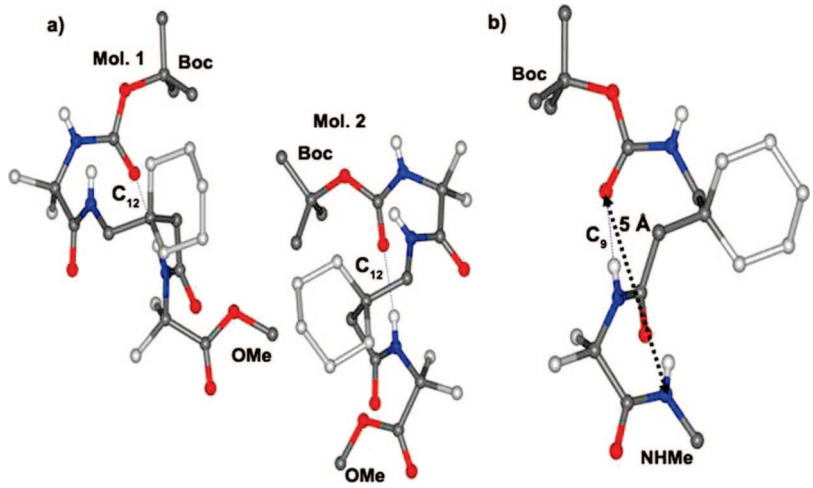

FIGURE 4. Molecular conformation determined in crystals of (a) Boc-Aib-Gpn-Aib-OMe (**5**) and (b) Boc-Gpn-Aib-NHMe (**6**).

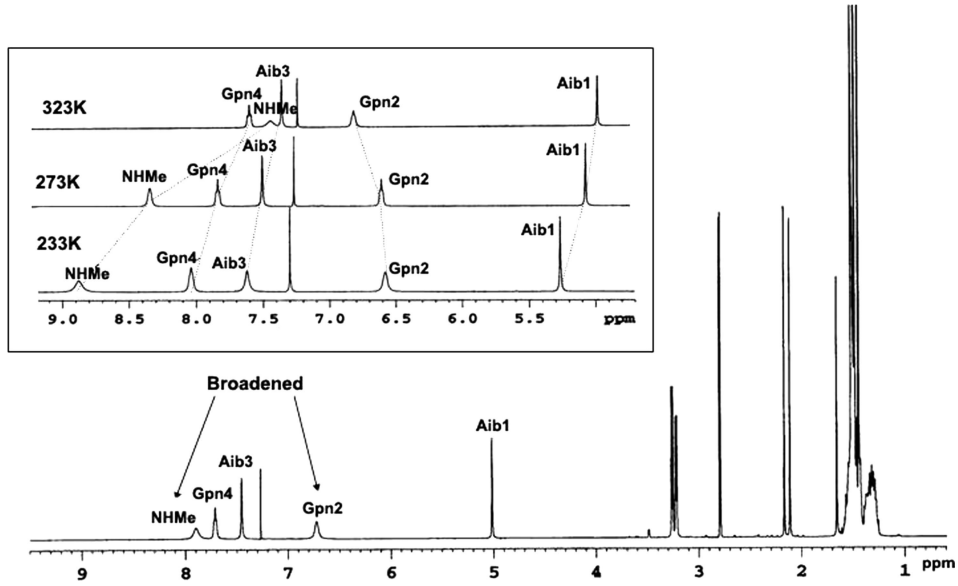

FIGURE 5. 500 MHz ^{1}H spectrum of Boc-Aib-Gpn-Aib-Gpn-NHMe (**2**) in $CDCl_3$ at 300 K. Inset shows the ^{1}H spectrum of **2** at 233, 273, and 323 K.

The delineation of the intramolecularly hydrogen-bonded (solvent shielded) NH groups in peptides can be conveniently accomplished by measuring the solvent dependence of the NH chemical shifts upon addition of a strongly hydrogen-bonding solvent like DMSO-d_6 or CD_3OH to a solution of apolar peptides in a poorly interacting solvent like $CDCl_3$.[9] Solvent-exposed NH groups show large downfield shifts upon addition of DMSO-d_6 to $CDCl_3$ solution of peptides. Buried and strongly hydrogen-bonded NH groups show little or no solvent dependence. The interpretation of solvent titration experiments in the case of systems which exhibit multiple conformational states must be approached cautiously. Figure 7a shows the amide NH resonances of peptide **2** in varying $CDCl_3$/DMSO-d_6 compositions. While the Gpn (2) and methylamide NH resonances are appreciably broadened in $CDCl_3$, addition of DMSO-d_6 results in a distinct broadening of the other three NH resonances. However, over the range of solvent compositions studied, only five distinct resonances are observed suggesting that the observed chemical shifts may only represent dynamically averaged values. The problem of unequal populations of the exchanging species is another factor that needs to be considered. Despite these caveats, the solvent titration curves shown in Figure 7b reveal that the NH groups of Aib (3), Gpn (4), and methylamide group show very little solvent dependence, suggestive of their involvement in intramolecular hydrogen bonding in the major species that are populated. This observation is consistent with both the continuous C_{12} helix (three hydrogen bonds) and also the conformation observed in crystals in the polymorph **2a**. Aib (1) NH behaves in the manner expected for a completely solvent exposed NH group. The diminished solvent sensitivity observed for the Gpn (2) NH resonance may be rationalized by contributions from conformations in which this residue adopts a C_7 hydrogen bonded structure (Gpn (2) NH$\cdots$Gpn (2) CO), a feature that is observed in the crystal structures of model Gpn peptides[5] (see also Gpn (4) of polymorphs **2b** and **2c** in Figure 2).

Solution Conformations of Nonapeptides Boc-Aib-Gpn-Aib-Gpn-Aib-Gpn-Aib-Gpn-Xxx-OMe. The conformational heterogeneity observed in the short $(\alpha\gamma)_n$ sequences prompted us to examine the effects of chain extension in the nonapeptides **3**

(9) (a) Pitner, T. P.; Urry, D. W. *J. Am. Chem. Soc.* **1972**, *94*, 1399–1400. (b) Iqbal, M.; Balaram, P. *J. Am. Chem. Soc.* **1981**, *103*, 5548–5552.

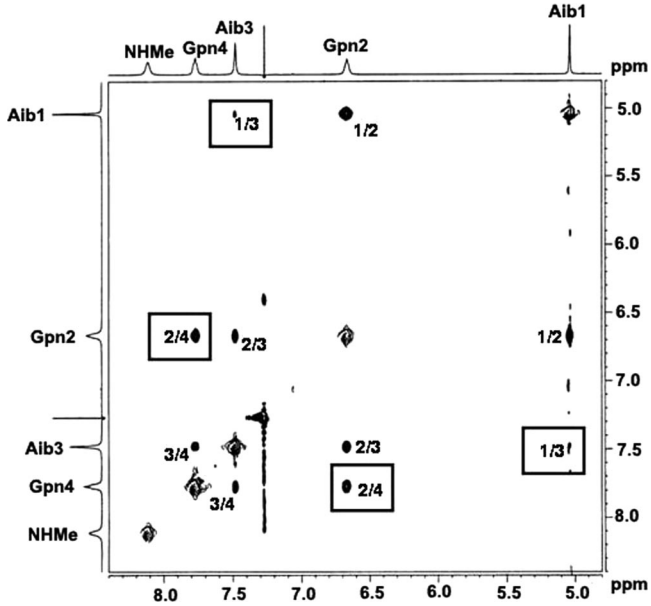

FIGURE 6. 500 MHz partial ROESY spectrum of Boc-Aib-Gpn-Aib-Gpn-NHMe (**2**) in $CDCl_3$ at 300K. Medium-range NOEs ($d_{NN[(i)\leftrightarrow(i+2)]}$) are highlighted (mixing time = 250 ms).

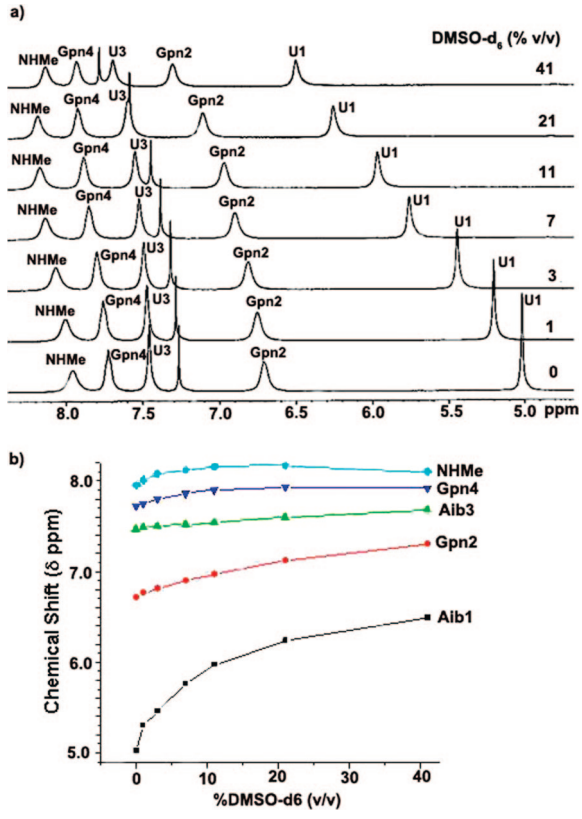

FIGURE 7. (a) Stacked ^1H spectrum of **2** at different solvent compositions ($CDCl_3$ + DMSO-d_6). (b) Plot of dependence of the NH chemical shifts of peptide **2** as a function of solvent composition ($CDCl_3$+ DMSO-d_6) (U = Aib).

(Xxx = Aib) and **4** (Xxx = ^{L}Leu). 500 MHz ^1H NMR spectrum of peptide **3** reveals well-dispersed NH resonances. Sequence-specific assignments were achieved using ROESY spectra, using the upfield position of the Aib (1) NH (urethane) as the starting point for establishing connectivity. The spectrum in Figure 8 reveals the selective broadening of Aib (3) and Gpn (4) NH groups. The ROESY spectrum illustrated in Figure 9 shows sequential connectivities between NH protons along the peptide backbone. Two d_{NN} NOEs, Aib (3) ↔ Gpn (4) and Gpn (4) ↔ Aib (5), are significantly weaker in intensities than the other NOEs. In an ideal helical C_{12} structure, the distances d_{NN} across the α and the γ residues are 2.7 and 3.4 Å, respectively (Figure 9). This should lead to a pattern of alternating d_{NN} NOE intensities. Inspection of Figure 9 reveals that the 1↔2, 5↔6, and 7↔8 NOEs ($d_{NN}(\alpha\gamma)$, across the α residues) are appreciably more intense than the 2↔3, 4↔5, 6↔7, and 8↔9 NOEs ($d_{NN}(\gamma\alpha)$, across the γ residues). In a robust, continuous C_{12} helix, a strong d_{NN} NOE between Aib (3) NH and Gpn (4) NH might have been anticipated. However, this NOE is very weak in the spectrum shown in Figure 9. Together with the observation of line broadening of Aib (3) NH and Gpn (4) NH resonances, the experimental findings suggest the possibility of conformational exchange processes involving the Aib (3) residue. It is pertinent to note that the Aib (3) residue in the tetrapeptide Boc-Aib-Gpn-Aib-Gpn-NHMe (**2**) adopts a polyproline II (P_{II}) conformation in both the crystalline polymorphs **2b** and **2c**. In a P_{II} conformation, the d_{NN} distance across the Aib residue is ~4.5 Å. It should be noted that unlike in the case of tetrapeptide **2**, no $d_{NN[i\leftrightarrow(i+2)]}$ NOEs are observed in the nonapeptide **3**. This suggests that lengthening of the $\alpha\gamma$ sequence favors population of the continuous C_{12} helical conformation. Further support for the continuous helical conformation in peptide **3** is obtained from a measurement of solvent dependence of NH chemical shifts in $CDCl_3$/DMSO-d_6 mixtures. The $\Delta\delta$ ($\delta_{(CDCl3+41.5\%DMSO\text{-}d6)} - \delta_{(CDCl3)}$, ppm) are as follows: Aib (1) NH 1.59, Gpn (2) NH 0.71, Aib (3) 0.19, Gpn (4) 0.25, Aib (5) −0.01, Gpn (6) 0.19, Aib (7) −0.03, Gpn (8) 0.05, Aib (9) −0.03. The higher $\Delta\delta$ values exhibited by Aib (1) NH and Gpn (2) NH indicate a significantly higher degree of solvent exposure compared to the other NH resonances, supporting a conformation in which the NH groups of residues 3−9 are involved in intramolecular hydrogen bonds. Heterogeneity of conformations in solution appears to be more pronounced in the case of short $\alpha\gamma$ sequences despite the backbone constraints inherent in the Aib and Gpn residues.

A nonapeptide sequence Boc-Aib-Gpn-Aib-Gpn-Aib-Gpn-Aib-Gpn-Leu-OMe (**4**) in which the terminal Aib has been replaced by the Leu was also synthesized in order to examine the effects of introduction of chirality on the C_{12} helix handedness facilitating future circular dichroism studies. The 500 MHz ^1H NMR spectra in $CDCl_3$ revealed that the distribution of backbone NH chemical shifts for residues 1−8 are almost identical to that observed for peptide **3**. The pattern of d_{NN} NOEs and their intensities and the solvent dependence of the NH chemical shifts are also almost identical to that described for peptide **3**. Interestingly, in this case also Aib (3) and Gpn (4) NH resonances showed evidence of selective broadening (see the Supporting Information).

Discussion

Hybrid polypeptide sequences incorporating backbone-homologated amino acid residues afford an opportunity to mimic the regular structures found in proteins or biologically active peptides, using non-α-amino acid residues. They provide new opportunities for exploring the relationships between the folded polymeric backbones and the nature of the intramolecular hydrogen bonds. Historically, the discovery of the α-helix and the β-sheet structures for the polypeptides by Pauling and

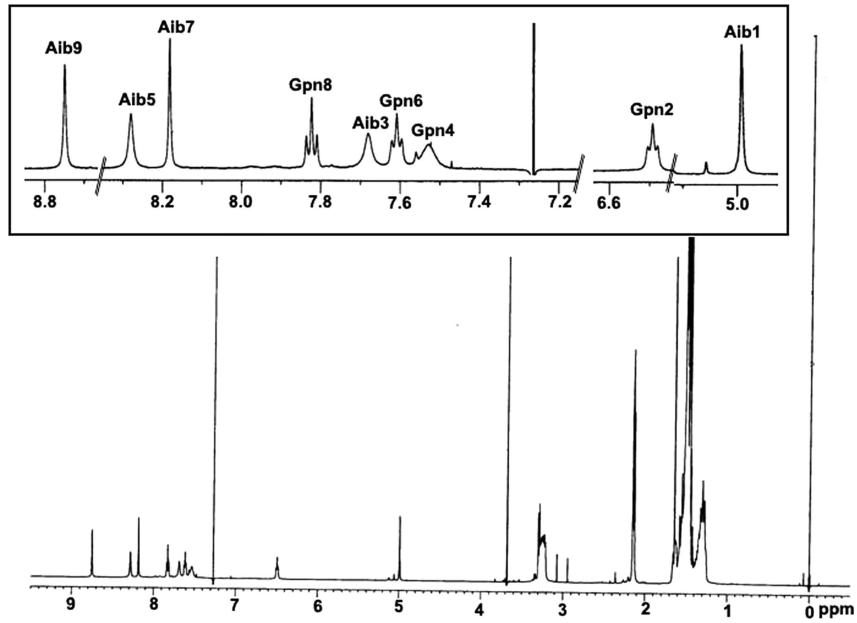

FIGURE 8. 500 MHz ^{1}H spectrum of nonapeptide Boc-Aib-Gpn-Aib-Gpn- Aib-Gpn-Aib-Gpn-Aib-NHMe (**3**) in $CDCl_3$ at 300 K. Inset shows the enlarged view of the amide region of the ^{1}H spectrum of **3**.

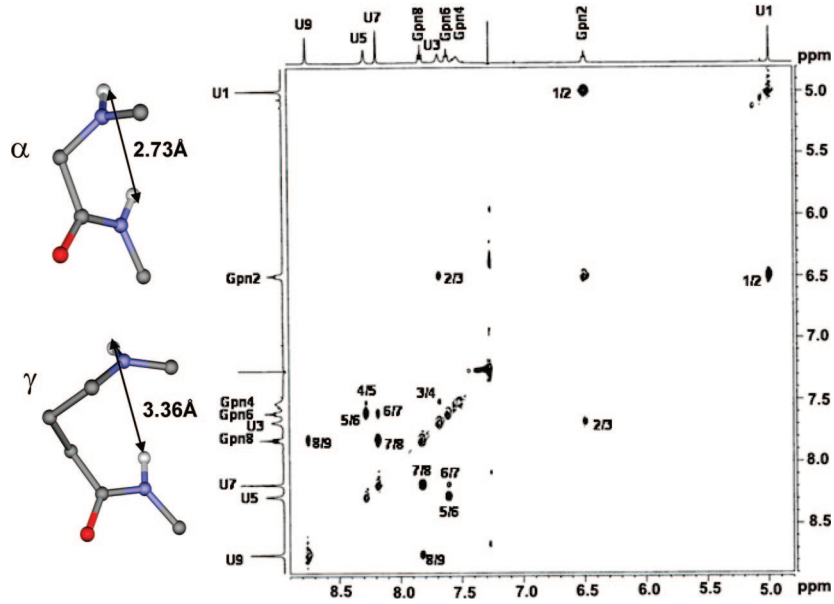

FIGURE 9. 500 MHz partial ROESY spectrum of peptide **3** in $CDCl_3$ at 300 K. On the left side are shown the d_{NN} distances across the α and γ residue (mixing time = 250 ms).

Corey[10] was based on an appreciation of the critical role of internal hydrogen bonds. The resurgence of interest in polypeptide structures follows the establishment of novel hydrogen bonding possibilities in oligomeric β-peptides.[3] The interest in foldamer design also stems from the fact that hybrid structures may be anticipated to be proteolytically more stable than their all-α counterparts.[3b,11] Our studies have been designed to examine conformational possibilities in regular $(\alpha\gamma)_n$ sequences using two conformationally constrained residues, Aib and Gpn. In the case of all-α amino acid backbones most of our understanding of hydrogen-bonded conformations has been derived from the vast body of structural information obtained from X-ray diffraction studies of natural proteins.[12] In contrast, information on hybrid sequences must necessarily be eked out by crystallographic and NMR studies of synthetic sequences. The interpretations of solution NMR data for short peptides are often uncertain, because of dynamic averaging over multiple conformational species. The use of backbone-constrained amino acids limits the range of conformational excursions permitting definitive characterization of specific folded structures.

(10) (a) Pauling, L.; Corey, R. B.; Branson, H. R. *Proc. Natl. Acad. Sci. U.S.A.* **1951**, *37*, 205–211. (b) Pauling, L.; Corey, R. B. *Proc. Natl. Acad. Sci. U.S.A.* **1951**, *37*, 729–740.

(11) Hook, D. F.; Bindschädler, P.; Mahajan, Y. R.; Šebesta, R.; Kast, P.; Seebach, D. *Chem. Biodiversity* **2005**, *2*, 591–632.

(12) (a) Baker, E. N.; Hubbard, R. E. *Prog. Biophys. Mol. Biol.* **1984**, *44*, 97–179. (b) Rose, G. D.; Gierasch, L. M.; Smith, J. A. *Adv. Protein Chem.* **1985**, *37*, 1–109. (c) Sibanda, B. L.; Thornton, J. M. *Nature* **1985**, *316*, 170–174. (d) Wilmot, C. M.; Thornton, J. M. *J. Mol. Biol.* **1988**, *203*, 221–232. (e) Richardson, J. S. *Adv. Protein Chem.* **1981**, *34*, 167–339.

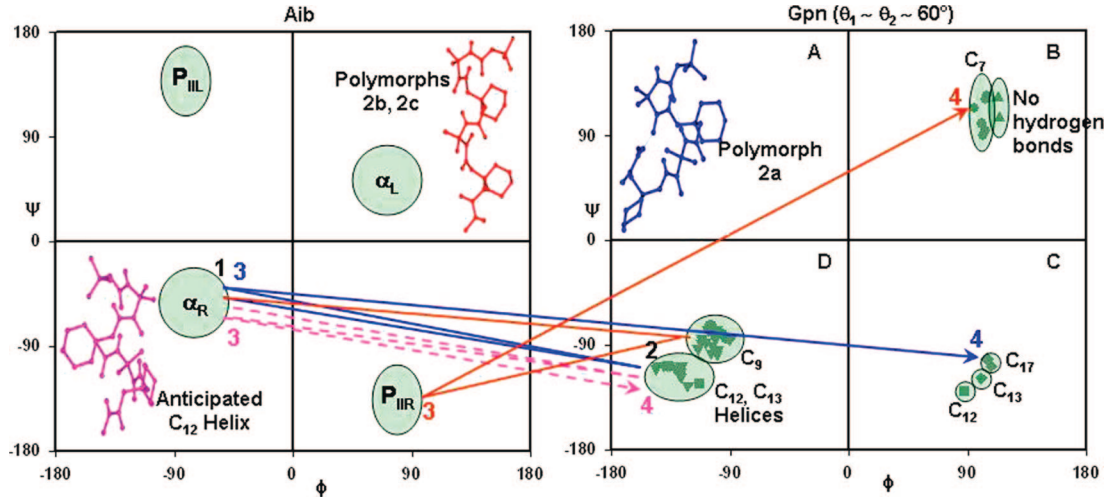

FIGURE 10. Representation of the backbone conformations of Aib and Gpn residues in the tetrapeptide **2** in ϕ,ψ space. The anticipated C_{12} helix (pink), the C_{12}/C_{17} structure in polymorph **2a** (blue), and the C_9/C_7 structure in polymorphs **2b** and **2c** (red) are shown. The experimentally observed conformational space for Aib and Gpn residues are marked with circles. The plot for Gpn (at $\theta_1 \approx \theta_2 \approx +60°$) includes 46 gabapentin residues from 25 peptides. The C_{13} and C_{12} circles in the quadrant C corresponds to the hydrogen bonded turns in C_{13}/C_{10} and C_{12}/C_{10} mixed helices with alternate hydrogen bond polarity. Lines connect linked residues in the peptide. Conformational transitions correspond to changes in the location of a given residue in the ϕ,ψ space. For all three structures, residues 1 and 2 (shown in black color) are in the same region of the conformational space. The lines and residue numbers follow the same color code as given for the structures.

For the achiral residue Aib, four distinct regions of the conformational space may be identified as potential energy minima. These are the helical α_R ($\phi = -60°$, $\psi = -30°$), the helical α_L ($\phi = +60°$, $\psi = +30°$), the polyproline P_{IIL} ($\phi = -60°$, $\psi = +120°$), and the polyproline P_{IIR} ($\phi = +60°$, $\psi = -120°$). In the case of this achiral residue, the pairs α_R/α_L and P_{IIL}/P_{IIR} are related by inversion about the origin of the $\phi-\psi$ map. The fully extended conformation ($\phi \approx \psi \approx 180°$) is not considered here as it does not lead to foldamers analogous to that in α amino acid structures.[13] For Aib, the helical conformations are overwhelmingly favored with only a small number of examples of P_{II} conformations being observed in peptide crystal structures.[14]

The γ residue, Gpn, provides two additional degrees of backbone torsional freedom. The positioning of the cyclohexyl substituent at the central C^β atom restricts the torsional degrees of freedom θ_1 ($C_\beta-C_\gamma$) and θ_2 ($C_\alpha-C_\beta$) to predominantly *gauche* conformations ($\theta_1 \approx \theta_2 \approx \pm 60°$), which are necessary for nucleating local folding. A body of crystal structures of short peptides determined in this laboratory has established the population of three distinct regions of $\phi-\psi$ space for fixed values of θ ($\theta_1 \approx \theta_2 \approx 60°$).[5,15] Figure 10 illustrates the observed Gpn conformations as cluster plots in $\phi-\psi$ space. In achiral peptides crystallizing in centrosymmetric space groups, symmetry-related molecules have inverted signs for all dihedral angles. The experimental values may then be represented by arbitrarily choosing one handedness. In the case of sequences containing chiral residues, the appropriate Gpn torsion angle signs can be chosen by considering an enantiomeric conformation. Interestingly, the C_9 ribbon observed in the $(\gamma)_n$ sequence, the C_{12} helix observed in $(\alpha\gamma)_n$ sequences and the C_{13} helix anticipated for the $(\beta\gamma)_n$ sequence[5a,16] lie in the same quadrant clustered in a limited region of the $\phi-\psi$ space. All three regular structures have the same hydrogen-bond directionality ($CO(i)\cdots NH(i+n)$) as in the regular α peptide helices (for all-α sequences, the corresponding helices are $n = 1$, 2.2_7 ribbon/helix (C_7); $n = 2$, 3_{10}-helix (C_{10}); $n = 3$, 3.6_{13}-helix (C_{13}). The $\alpha\gamma$ C_{12} turn and the $\beta\gamma$ C_{13} turn[5a] clustered in the quadrant C are expanded analogues of the "non-helical" β-turns observed in isolated two-residue all-α-segments. These are "non-helical" turns which provide a means of reversing polypeptide chain directionality, commonly facilitating β-hairpin structures.[4c,17] In the three-residue $\gamma\alpha\gamma$ C_{17} hydrogen-bonded structure observed in the tetrapeptide Boc-Aib-Gpn-Aib-Gpn-NHMe in the polymorph **2a**, Gpn (4) lies in quadrant C, while Gpn (2) is in quadrant D. This conformational feature brings the C^α of the two flanking residues to a distance of 5.2 Å, which is strikingly similar to that observed for the hairpin nucleating type II′ β-turn.[18] Thus, both helix and hairpin promoting turns may be readily generated with $\alpha\gamma$ hybrid segments. Quadrant B contains a cluster of C_7 hydrogen-bonded structures of Gpn residues and two examples of non-hydrogen-bonded Gpn residues which are very close to the C_7 conformation. The C_7 structure is an expanded version of the C_5 structure proposed for the fully extended α polypeptides.[4f,13] While the C_5 hydrogen bond in the α residues is characterized by an extremely unfavorable NH···O angle of 90°, the parameters for the C_7 hydrogen bond are more favorable (N···O = 2.97 Å, H···O = 2.35 Å, ∠N−H···O = 130.5°).[5a] The C_7 conformation corresponds to a change in hydrogen bond directionality ($NH(i)\cdots CO(i+n)$);

(13) (a) Toniolo, C.; Benedetti, E. In *Molecular Conformation and Biological Interactions*; Balaram, P., Ramaseshan, S. Eds.; Indian Academy of Sciences: Bangalore, India, 1991; pp 511−521. (b) Toniolo, C. *CRC Crit. Rev. Biochem.* **1980**, *9*, 1–44.

(14) (a) Aravinda, S.; Shamala, N.; Balaram, P. *Chem. Biodiversity* **2008**, . in press. (b) In a total of 1385 Aib residues characterized in peptide crystals, 1315 residues are helical (α_L or α_R) and 61 residues are in the P_{II} region of the ϕ,ψ space.

(15) (a) Aravinda, S.; Ananda, K.; Shamala, N.; Balaram, P. *Chem. Eur. J.* **2003**, *9*, 4789–4795. (b) Vasudev, P. G.; Shamala, N.; Ananda, K.; Balaram, P. *Angew. Chem., Int. Ed.* **2005**, *44*, 4972–4975.

(16) The $\beta\gamma$ helical C_{13} turn was observed in the tripeptide Boc-βLeu-Gpn-Val-OMe (refs 1a and 5a).

(17) (a) Hughes, R. M.; Waters, M. L. *Curr. Opin. Struct. Biol.* **2006**, *16*, 514–524. (b) Rai, R.; Raghothama, S.; Balaram, P. *J. Am. Chem. Soc.* **2006**, *128*, 2675–2681, and references therein.

(18) The average $C^\alpha-C^\alpha$ distance for residues flanking hairpin nucleating type II′ β-turns ($C^\alpha(i)\cdots{}^\alpha(i+3)$, where $i+1$ and $i+2$ are the turn residues) determined from analysis of eight peptide hairpin crystal structures is 5.1 Å.

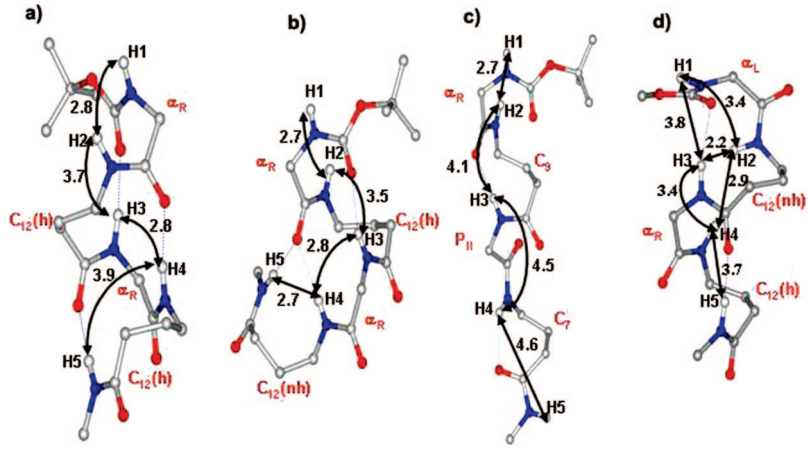

FIGURE 11. d_{NN} distances in different conformations of peptide **2**: (a) the anticipated C_{12} helix; (b) C_{12} helix terminated with C_{17} turn determined in the crystals of polymorph **2a**; (c) C_9/C_7 conformation observed in polymorphs **2b** and **2c** (in this conformation, the only distance corresponding to an observable NOE is $d_{H1\leftrightarrow H2}$); (d) model conformation which explains the 2↔4 and 1↔3 NOEs in the tetrapeptide **2**. Residue conformations are indicated. C_{12} (nh) and C_{12} (h) correspond to the helical and nonhelical C_{12} conformations of Gpn in quadrants C and D, respectively, in Figure 10. (The 1↔3 and 2↔4 distances in parts a−c are as follows: (a)/(b) ≈ 4.6 Å; (c) 1↔3 ≈ 5.7, 2↔4 ≈ 8.5 Å.)

for the C_7 structure, $n = 0$) which is a reversal of that observed in α polypeptide structures. In $(\alpha\gamma)_n$ sequences, reversal of hydrogen bond polarity has been observed resulting in C_{10} turns where $n = 1$. Indeed, a novel regular structure consisting of successive C_{12} (CO(i)···HN(i+3), normal direction) and C_{10} (NH(i)···OC(i+1), opposite direction) hydrogen bonds can be generated in a repetitive $(\alpha\gamma)_n$ sequence resulting in a $C_{12}-C_{10}$ helical structure. Such a structure has been postulated on the basis of theoretical calculations[1f] and observed in the structure of the tetrapeptide Boc-Leu-Gpn-Leu-Aib-OMe, in which the Leu residue adopts a P_{II} conformation and the Gpn residue is in the nonhelical C_{12} conformation, falling in quadrant C (unpublished results). From Figure 10, it is seen that the polymorphs of Boc-Aib-Gpn-Aib-Gpn-NHMe **2a**, **2b**, and **2c** and the continuous $\alpha\gamma$ C_{12} helix are all generated by local residue conformations, which lie in a limited region of $\phi-\psi$ space for both Aib and Gpn residues. Despite the high degree of local conformational selection in these constrained residues, a high degree of structural heterogeneity is possible in these $\alpha\gamma$ hybrid sequences. It is evident that the transitions of Gpn (4) between the quadrants B, C and D may indeed require the crossing of appreciable activation barriers.

The multiplicity of accessible conformations is most evident in the shorter sequences, for example, in peptide **2**. While some conformations may be captured in crystals, evidence for other states begins to appear in NOE studies. In particular, the interproton NOE between NH(i) and NH(i+2) is a clear diagnostic of the presence of conformations other than the continuous C_{12} helix. The measured short d_{NN} distances in the two distinct polymorphic forms observed in crystals are shown in Figure 11. In short peptide sequences, NOEs up to 3.5−4.0 Å are detectable, although there is a sharp fall in intensities for interproton distances greater than 3.5 Å. It is evident from Figure 11 that in the conformations **2a**−**c** no $d_{NN[i\leftrightarrow(i+2)]}$ NOEs are likely to be observed. Figure 11d illustrates a model conformation constructed by choosing local residue conformations within the experimentally observed regions of $\phi-\psi$ space depicted in Figure 10. For an $\alpha\gamma$ sequence forming a nonhelical C_{12} turn, the $d_{NN[(i)\leftrightarrow(i+2)]}$ distance is approximately 3.8 Å. Notably, the H(1)↔H(3) NOE in Figure 6 is extremely weak. Interestingly, when the γ residue in a C_{12} nonhelical conformation is followed by an α residue in a helical conformation, the NH(4) is left free, resulting in the absence of a C_{12} hydrogen bond in the segment, but yields a short H(2)↔H(4) distance of 2.9 Å and brings H(2) and H(3) as close as 2.2 Å. Interestingly, H(2)↔H(4) NOEs observed in Figure 6 are of significantly greater intensities than the H(1)↔H(3) NOE. In the case of peptide **2**, the NOE data strongly suggests the presence of multiple conformational states, which are distinct from the conformations characterized in crystals. In such a situation, the interpretations of the NOE intensities are fraught with uncertainty. Small populations of conformations with short interproton distances can contribute significantly to the observed NOEs. The absence or weakness of a particular NOE cannot be interpreted in terms of a specific solution conformation.[19]

Lengthening of the polypeptide chain in the nonapeptides **3** and **4** appears to result in nucleation and stabilization of the regular $\alpha\gamma$ C_{12} helix. In these cases, the alternating pattern of intensities of the sequential d_{NN} NOEs across the α and γ residues provides a clear signature of the C_{12} helical conformation. The chain length dependence of helix formation in all-α peptides is a well-established phenomena.[20] The present studies indicate that continuous helix formation in hybrid $\alpha\gamma$ sequences can also be facilitated by the lengthening of the peptide chain. The design of repetitive hybrid $(\alpha\gamma)_n$ peptides using residues with limited conformational choices, Aib and Gpn, was undertaken to establish the diversity of intramolecularly hydrogen-bonded structures in these sequences. The characterization of the C_{12} helix and the observation of the $\gamma\alpha\gamma$ C_{17} hydrogen bonded turn illustrate examples of hydrogen-bonded hybrid structures, which are potentially capable of mimicking secondary structural features in all-α peptides. The area of hybrid peptide design using γ-amino acid residues will undoubtedly receive further impetus from the introduction of novel backbone modified residues using newly developed synthetic methodologies.[21]

(19) Neuhaus, D.; Williamson, M. P. *The Nuclear Overhauser Effect in Structural and Conformational Analysis*; Wiley-VCH: New York, 2000.

(20) (a) Goodman, M.; Verdini, A. S.; Toniolo, C.; Phillips, W. D.; Bovey, F. A. *Proc. Natl. Acad. Sci. U.S.A.* **1969**, *64*, 444–450. (b) Scholtz, J. M.; Baldwin, R. L. *Ann. Rev. Biophys. Biomol. Struct.* **1992**, 95–118. (c) Fiori, W. R.; Miick, S. M.; Millhauser, G. L. *Biochemistry* **1993**, *32*, 11957–11962.

(21) Chi, Y.; Guo, L.; Kopf, N. A.; Gellman, S. H. *J. Am. Chem. Soc.* **2008**, *130*, 5608–5609.

Experimental Procedures

Peptide Synthesis and Characterization. Peptide synthesis was carried out using conventional solution-phase procedures.[22] The details of the synthesis are discussed below.

(A) Boc-Aib-Gpn-Aib-Gpn-NHMe (2). (i) Boc-Gpn-NHMe.[5b] Boc-Gpn-OH (2.7 g, 10 mmol) was dissolved in 10 mL of dry THF (tetrahydrofuran) and cooled in an ice bath while stirring. Et_3N (1.3 mL, 10 mmol) and EtOCOCl (1.3 mL, 10 mmol) were added into the reaction mixture. Thirty milliliters of dry THF saturated with methylamine gas was added. The reaction mixture was left undisturbed overnight. The solvent was evaporated and the residue dissolved in ethyl acetate. The organic layer was washed successively with brine (3 × 30 mL), 2 N HCl (3 × 30 mL), 1 M sodium carbonate (3 × 30 mL), and brine. This layer was dried over anhydrous sodium sulfate and evaporated in vacuo to yield Boc-Gpn-NHMe (2.3 g, 80%) as a white solid.

(ii) Boc-Aib-Gpn-NHMe. Boc-Gpn-NHMe (2.3 g, 8 mmol) was deprotected with 40 mL of 98% formic acid, and the deprotection was monitored by TLC. After 2 h, formic acid was evaporated; the residue was taken in 10 mL of water. The pH of the aqueous layer was adjusted to ∼8 by addition of sodium carbonate and extracted with ethyl acetate (3 × 30 mL). The combined organic layer was washed with brine solution (30 mL) and concentrated in vacuo to ∼2 mL. The peptide-free base was added to a precooled solution of 1.6 g (8 mmol) of Boc-Aib-OH in 5 mL of dry THF followed by addition of 1.6 g (8 mmol) of DCC (*N*,*N*′-dicyclohexylcarbodiimide) and 1.2 g of HOBT (1-hydroxybenzotriazole). The reaction mixture was allowed to attain room temperature and was stirred for 2 days. The reaction was worked up as described in (i). Boc-Aib-Gpn-NHMe (2.6 g, 87.5%) was obtained as a white solid and used for synthesis without further purification. ESI-MS, MH^+_{obsd} (MH^+_{calcd}) Da: 369.5 (369).

(iii) Boc-Aib-Gpn-OH.[23] Boc-Aib-OH (2.0 g, 10 mmol) was dissolved in 10 mL of dry THF and cooled in an ice bath. HOSu (2.0 g, 17.4 mmol) followed by 2.0 g (10 mmol) of DCC was added. The reaction mixture was allowed to attain room temperature. After 12 h, the DCU (*N*,*N*′-dicyclohexylurea) was filtered off, and the filtrate was washed with brine (3 × 30 mL), 1 M sodium carbonate (3 × 30 mL), and brine (1 × 30 mL). The organic layer was dried over sodium sulfate and evaporated in vacuo. Boc-Aib-OSu (2.7 g, 90%) was obtained as a white solid. Boc-Aib-OSu (2.7 g, 9 mmol) was dissolved in 10 mL of THF followed by addition of 20% sodium carbonate solution and 2.4 g (9 mmol) of H-Gpn-OH. The reaction was stirred for 24 h at room temperature. THF was evaporated, and the residue was taken in 20 mL of water and was washed with 30 mL of ethyl acetate. The aqueous layer was acidified with 2 N HCl and was extracted with ethyl acetate (3 × 30 mL). The pooled organic layer was washed with brine (30 mL) and was dried over sodium sulfate and was evaporated in vacuo. Boc-Aib-Gpn-OH (2.8 g, 88.9%) was obtained as a white solid and used without further purification. ESI-MS, MH^+_{obsd} (MH^+_{calcd}) Da: 356.5 (356).

(iv) Boc-Aib-Gpn-Aib-Gpn-NHMe (2). Boc-Gpn-Aib-NHMe (2.6 g, 7 mmol) was deprotected with 35 mL of 98% formic acid, and the deprotection was monitored by TLC. After 3 h, formic acid was evaporated, and the residue was taken in 10 mL of water. The pH of the aqueous layer was adjusted to ∼8 by addition of sodium carbonate and extracted with ethyl acetate (3 × 30 mL). The combined organic layer was washed with brine solution (30 mL) and concentrated in vacuo to ∼2 mL. The dipeptide-free base was added to a precooled solution of 2.5 g (7 mmol) of Boc-Aib-Gpn-OH in 5 mL of dry THF followed by addition of 1.4 g (7 mmol) of DCC and 1.0 g (7 mmol) of HOBT. The reaction mixture was allowed to attain room temperature and was stirred for 2 days. The reaction was worked up as detailed in (i). Boc-Aib-Gpn-Aib-Gpn-NHMe **2** (3.0 g, 71%) was obtained as a white solid.

Peptide **2** was purified by reversed-phase, medium-pressure liquid chromatography (C_{18}, 40−60 μm) and high-performance liquid chromatography (HPLC) on a reversed-phase C_{18} column (5−10 μm, 7.8−250 mm) using methanol/water gradients. ESI-MS, MH^+_{obsd} (MH^+_{calcd}) Da: 608.5 (608). Peptide identity was also confirmed by complete assignment of 500 MHz ^{1}H NMR spectra.

(B) Boc-Aib-Gpn-Aib-Gpn-Aib-Gpn-Aib-Gpn-Aib-OMe (3). (i) Boc-Aib-Gpn-Aib-OMe. Boc-Aib-Gpn-Aib-OMe was synthesized by coupling 3.5 g (10 mmol) of Boc-Aib-Gpn-OH obtained as discussed in section A(iii) to H-Aib-OMe obtained from 3.0 g (20 mmol) of H-Aib-OMe hydrochloride, upon neutralization, extraction, and concentration using DCC/HOBT as coupling agents. The reaction was worked up as in section A(iv) to yield the tripeptide (3.6 g, 80%) as a white solid. ESI-MS, MH^+_{obsd} (MH^+_{calcd}) Da: 455.5 (455). The peptide was used for synthesis without purification.

(ii) Boc-Aib-Gpn-Aib-Gpn-Aib-OMe. Boc-Aib-Gpn-Aib-OMe (3.6 g, 8 mmol) was deprotected with 40 mL of 98% formic acid and was worked up as in section A(iv). The free base was added to a precooled solution of 2.8 g (8 mmol) of Boc-Aib-Gpn-OH, obtained as in section A(iii), in 5 mL of dry THF followed by addition of 1.6 g (8 mmol) of DCC and 1.2 g (8 mmol) of HOBT. The reaction mixture was allowed to attain room temperature and was stirred for 2 days. The reaction was worked up as described in section A(iv). Boc-Aib-Gpn-Aib-Gpn-Aib-OMe was obtained as a white solid (4.8 g, 87.5%), which was used for synthesis without further purification. ESI-MS, MH^+_{obsd} (MH^+_{calcd}) Da: 693.5 (693).

(iii) Boc-Aib-Gpn-Aib-Gpn-Aib-Gpn-Aib-OMe. Boc-Aib-Gpn-Aib-Gpn-Aib-OMe (4.8 g, 7 mmol) was deprotected with 35 mL of 98% formic acid, and the reaction was worked up as discussed in section A(iv). The free base was added to a precooled solution of 2.5 g (7 mmol) of Boc-Aib-Gpn-OH, obtained as in section A(iii), in 5 mL of dry THF followed by addition of 1.4 g (7 mmol) of DCC and 1.0 g (7 mmol) of HOBT. The reaction mixture was allowed to attain room temperature and was stirred for 5 days. The reaction was worked up as in section A(iv) above. Boc-Aib-Gpn-Aib-Gpn-Aib-Gpn-Aib-OMe (4.8 g, 71%) was obtained as a white solid, which was used for synthesis without further purification. ESI-MS, MH^+_{obsd} (MH^+_{calcd}) Da: 931.5 (931).

(iii) Boc-Aib-Gpn-Aib-Gpn-Aib-Gpn-Aib-Gpn-Aib-OMe (3). Boc-Aib-Gpn-Aib-Gpn-Aib-Gpn-Aib-OMe (4.6 g, 5 mmol) was deprotected with 25 mL of 98% formic acid and reaction was worked up as discussed in section A(iv). The free base was added to a precooled solution of 1.8 g (5 mmol) of Boc-Aib-Gpn-OH, obtained as in section A(iii), in 5 mL of dry THF followed by addition of 1.0 g (5 mmol) of DCC and 0.8 g (5 mmol) of HOBT. The reaction mixture was allowed to attain room temperature and was stirred for 5 days. The reaction was worked up as in section A(iv). Boc-Aib-Gpn-Aib-Gpn-Aib-Gpn-Aib-Gpn-Aib-OMe **3** (3.9 g, 60%) was obtained as a white solid.

Peptide **3** was purified by reversed-phase, medium-pressure liquid chromatography (C_{18}, 40 − 60 μm) and high-performance liquid chromatography (HPLC) on a reversed-phase C_{18} column (5−10 μm, 7.8−250 mm) using methanol/water gradients. ESI-MS, MH^+_{obsd} (MH^+_{calcd}) Da: 1169.5 (1169). Peptide identity was also confirmed by complete assignment of 500 MHz ^{1}H NMR spectra.

(C) Boc-Aib-Gpn-Aib-Gpn-Aib-Gpn-Aib-Gpn-Leu-OMe (4). (i) Boc-Aib-Gpn-Leu-OMe. Boc-Aib-Gpn-Leu-OMe was synthesized by coupling 3.5 g (10 mmol) of Boc-Aib-Gpn-OH obtained as discussed in section A(iii), to H-Leu-OMe obtained from 3.6 g (20 mmol) H-Leu-OMe hydrochloride upon neutralization, extraction, and concentration using DCC/HOBT as coupling agents. The reaction was worked up as in section A(iv). The tripeptide was

(22) Bodanszky, M.; Bodanszky, A. *The Practice of Peptide Synthesis*; Springer-Verlag: Berlin, 1984.

(23) Aravinda, S.; Ananda, K.; Shamala, N.; Balaram, P. *Chem. Eur. J.* **2003**, *9*, 4789–4795.

(24) (a) Schneider, T. R.; Sheldrick, G. M. *Acta Crystallogr.* **2002**, *D58*, 1772–1779. (b) Sheldrick, G. M. *SHELXS-97, A program for automatic solution of crystal structures*; University of Göttingen: Göttingen, 1997. (c) Sheldrick, G. M. *SHELXL-97, A program for crystal structure refinement*; University of Göttingen: Göttingen, 1997.

TABLE 3. Crystal and Diffraction Parameters for Boc-Aib-Gpn-Aib-Gpn-NHMe (2), Boc-Aib-Gpn-Aib-OMe (5), and Boc-Gpn-Aib-NHMe (6)

	2a	2b	2c	5	6
empirical formula	C_{32} H_{57} N_5 O_6	C_{32} H_{57} N_5 O_6. H_2O. (0.25) CH_3OH	C_{32} H_{57} N_5 O_6. H_2O	C_{23} H_{41} N_3 O_6	C_{19} H_{35} N_3 O_4
crystal habit	small needle	rhombus-shaped plates	rhombus-shaped plates	plates	plates
crystallizing solvent	ethyl acetate/hexane/methanol	methanol/water/dioxane	methanol	methanol/water	methanol/water
crystal size (mm)	0.20 × 0.03 × 0.01	0.6 × 0.5 × 0.14	0.2 × 0.09 × 0.07	0.25 × 0.04 × 0.02	0.5 × 0.04 × 0.02
space group	$P2_1/c$	$P2_1/c$	$P2_1/c$	$P2_1/c$	$P2_1/c$
a (Å)	17.447(4)	14.462(1)	10.276(2)	16.892(1)	9.978(2)
b (Å)	11.722(3)	13.179(1)	12.307(2)	16.436(1)	20.950(4)
c (Å)	35.799(9)	20.322(1)	30.071(2)	18.990(1)	11.043(2)
β (deg)	96.50(1)	104.416(1)	105.896(3)	92.128(1)	110.464(3)
volume (Å^3)	7274(3)	3734.0(5)	3657.4(11)	5268.8(3)	2162.9(6)
Z	8	4	4	8	4
molecules/asym unit	2	1	1	2	1
co-crystallized solvent	none	1 water + 0.25 methanol	water	none	none
formula wt	607	632.8	625.8	455.5	369.5
density (g/cm^3) (cal)	1.11	1.13	1.14	1.15	1.13
F (000)	2656	1382	1368	1984	808
2θ Max. (°)	46.5	53.6	50.7	53.1	49.4
measured reflns	44479	27608	25443	38312	14763
R_{int}	0.34	0.022	0.10	0.067	0.035
unique reflns	10424	7362	6634	10048	3676
obsd reflns [$\|F\| > 4\sigma(F)$]	2397	5348	3348	4605	3048
final R (%)/wR2 (%)	8.92/10.62	4.97/13.85	8.08/15.01	7.96/16.28	8.95/25.26
goodness-of-fit (S)	0.884	0.974	1.03	1.008	1.165
$\Delta\rho_{max}$ (e Å^3)/$\Delta\rho_{min}$ (e Å^{-3})	0.33/−0.19	0.27/−0.14	0.25/−0.20	0.21/−0.14	0.47/−0.23
restraints/parameters	9/755	0/443	0/425	0/577	0/247
data-to-parameter ratio	4:1	12:1	8:1	8:1	12:1

obtained as a white solid (3.9 g, 80%), which was used for further synthesis without purification. ESI-MS, MH^+_{obsd} (MH^+_{calcd}) Da: 483.5(483).

(ii) Boc-Aib-Gpn-Aib-Gpn-Leu-OMe. Boc-Aib-Gpn-Leu-OMe (3.9 g, 8 mmol) was deprotected with 40 mL of 98% formic acid and was worked up as in section A(iv). The free base was added to a precooled solution of 2.8 g (8 mmol) of Boc-Aib-Gpn-OH, which was obtained as in section A(iii), in 5 mL of dry THF followed by addition of 1.6 g (8 mmol) of DCC and 1.2 g (8 mmol) of HOBT. The reaction mixture was allowed to attain room temperature and was stirred for 3 days. The reaction was worked up as in section A(iv). Boc-Aib-Gpn- Aib-Gpn-Leu-OMe (4.3 g, 75%) was obtained as a white solid, which was used for synthesis without further purification. ESI-MS, MH^+_{obsd} (MH^+_{calcd}) Da: 721.5 (721).

(iii) Boc-Aib-Gpn-Aib-Gpn-Aib-Gpn-Leu-OMe. Boc-Aib-Gpn-Aib-Gpn-Leu-OMe (4.3 g, 6 mmol) was deprotected with 30 mL of 98% formic acid, and the reaction was worked up as discussed in section A(iv). The free base was added to a precooled solution of 2.1 g (6 mmol) of Boc-Aib-Gpn-OH, obtained as in section A(iii), in 5 mL of dry THF followed by addition of 1.2 g (6 mmol) of DCC and 0.9 g (6 mmol) of HOBT. The reaction mixture was allowed to attain room temperature and was stirred for 5 days. The reaction was worked up as in section A(iv). Boc-Aib-Gpn-Aib-Gpn-Aib-Gpn-Leu-OMe (4.7 g, 83%) was obtained as a white solid, which was used for synthesis without further purification. ESI-MS, MH^+_{obsd} (MH^+_{calcd}) Da: 959.5 (959).

(iv) Boc-Aib-Gpn-Aib-Gpn-Aib-Gpn-Aib-Gpn-Leu-OMe (4). Boc-Aib-Gpn-Aib-Gpn-Aib-Gpn-Leu-OMe (4.7 g, 5 mmol) was deprotected with 25 mL of 98% formic acid, and the reaction was worked up as discussed in section A(iv). The free base was added to a precooled solution of 1.8 g (5 mmol) of Boc-Aib-Gpn-OH, obtained as in section A(iii), in 5 mL of dry THF followed by addition of 1.0 g (5 mmol) of DCC and 0.8 g (5 mmol) of HOBT. The reaction mixture was allowed to attain room temperature and was stirred for 7 days. The reaction was worked up as in section A(iv), to yield Boc-Aib-Gpn-Aib-Gpn-Aib-Gpn-Aib-Gpn-Leu-OMe **4** (2.4 g, 40%) as a white solid.

Peptide **4** was purified by reversed-phase, medium-pressure liquid chromatography (C_{18}, 40 − 60 μm) and high-performance liquid chromatography (HPLC) on a reversed-phase C_{18} column (5−10 μm, 7.8−250 mm) using methanol/water gradients. ESI-MS, MH^+_{obsd} (MH^+_{calcd}) Da: 1197.5 (1197). Peptide identity was also confirmed by complete assignment of 500 MHz ^{1}H NMR spectra.

(D) Boc-Aib-Gpn-Aib-OMe (5) and Boc-Gpn-Aib-NHMe (6). Peptide **5** was synthesized as discussed in section B(i). Peptide **6** was synthesized by coupling Boc-Gpn-OH (2.71 g, 10 mmol) to Aib-NHMe, obtained by deprotecting Boc-Aib-NHMe, (2.2 g, 10 mmol) using DCC (2 g,10 mmol)/HOBT (1.5 g,10 mmol) as the coupling agents. The final peptides were purified by reversed phase, medium-pressure liquid chromatography (C_{18}, 40−60 μm) using methanol/water gradients. ESI-MS, MH^+_{obsd} (MH^+_{calcd}) Da: **5**, 455.7 (455); **6**, 370.5 (370).

NMR Spectroscopy. All proton NMR spectra were recorded at 500 MHz. Chemical shifts are reported with respect to internal tetramethylsilane (TMS). Peptide concentrations used are as follows: peptide **2**, 3.7 mM; peptides **3** and **4**, 1.9 mM. Aggregation effects for peptides at these concentrations are not significant in the solvents used. Sequence specific assignments were readily achieved, since the Aib (1) NH (urethane NH) can be unambiguously identified by its high-field position. The singlet and triplet appearances of Aib and Gpn NH, respectively, together with sequential NOEs, permit unambiguous assignment. The nuclear Overhauser effects (NOE) were observed using ROESY experiments employing standard pulse sequences from a manufacturer's library. A single mixing time (CW spin lock time) of 250 ms was used.

Crystal Structure Determination. Three polymorphic forms of peptide **2**, Boc-Aib-Gpn-Aib-Gpn-NHMe were obtained by slow evaporation from different solvent mixtures. The peptide, when crystallized independently from an ethyl acetate/hexane/methanol mixture and from a methyl acetate/hexane mixture, yielded small needles (polymorph **2a**). Crystallization of a fresh sample of peptide **2** from a methanol/water/dioxane mixture yielded rhombus-shaped single crystals (polymorph **2b**). The crystals of the third polymorph (**2c**), obtained by slow evaporation from methanol, resembled the **2b** crystals, but were thinner. All three polymorphs crystallized in the monoclinic space group $P2_1/c$. The asymmetric unit of polymorph **2a** is composed of two independent peptide molecules. Polymorph **2b** crystallized along with a molecule of water and a partially occupied (0.25) methanol molecule in the asymmetric unit, while peptide **2c** crystallized along with a lone water molecule in the asymmetric unit. Peptides **5** and **6** were obtained from methanol/water mixture by slow evaporation, in monoclinic space group $P2_1/c$. Peptide **5** has two molecules in the asymmetric unit, while **6**

crystallized with one molecule in the asymmetric unit. X-ray intensity data for all crystals were collected at room temperature on a CCD diffractometer (Mo Kα radiation, $\lambda = 0.71073$ Å, ω-scan). The structures were solved by direct methods using SHELXD[24a] (**2a**) or SHELXS-97[24b] (**2b**, **2c**, **5**, **6**) and refined against F,[2] with full-matrix least-squares methods using SHELXL-97.[24c] The rest of the hydrogen atoms in **2b**, **2c**, and **6** and all of the hydrogen atoms for **2a** and **5** were fixed geometrically in idealized positions and were refined as riding over the atoms to which they were bonded. During the refinement, restraints were applied on bond lengths and bond angles of Gpn (2) side chain of Mol. Two in polymorph **2a**, in order to maintain an acceptable geometry of the cyclohexane ring. Poor crystal quality limits the diffraction data to 0.9 Å resolution, resulting in large thermal ellipsoids for the carbon atoms of the Gpn (2) side chain. Table 3 summarizes the crystal and diffraction parameters for peptides **2**, **5**, and **6**.

Acknowledgment. This research was supported by a grant from the Council of Scientific and Industrial Research (CSIR) and Program Support in the area of Molecular Diversity and Design, Department of Biotechnology, India. We thank Dr. K. Nagarajan of Hikal R&D Centre, Bangalore (India), for the sample of gabapentin. S.C. and P.G.V. thank the CSIR for Senior Research Fellowships. X-ray diffraction data were collected at the CCD facility funded under the IRHPA program of the Department of Science and Technology, India.

Supporting Information Available: X-ray crystallographic information files for peptides **2**, **5**, and **6** (CIF), chemical shifts of amide NH resonances for peptides **3** and **4** (Table S1), ^{1}H NMR and ROESY spectra of peptide **4**, solvent titration plots for peptides **3** and **4** (Figures S1−S4). This material is available free of charge via the Internet at http://pubs.acs.org. The X-ray crystallographic files (CIF) have also been deposited with the Cambridge Structural Database with accession numbers CCDC 663392−663394 (**2a**−**2c**), 684733 (**5**), and 684734 (**6**).

JO8009819